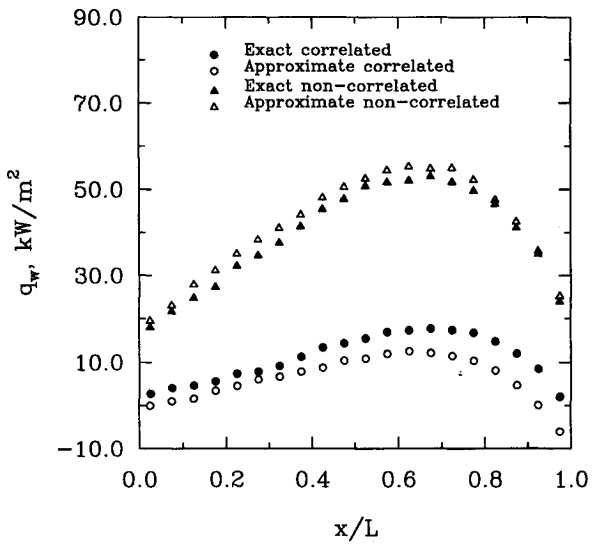

Fig. 3 Radiative wall flux distributions for nonisothermal and inhomogeneous H_2O-O_2-N_2 mixture.

bution in the medium and much higher radiative wall flux along the plates than the correlated formulations. This difference comes from the statistical relationship for determining the absorption location. The R_l calculated from the noncorrelated formulation, Eq. (9), is greater than that from the correlated formulations, Eqs. (8) and (13). Therefore, for the noncorrelated formulation, an energy bundle travels a long distance and is likely to be absorbed on the wall. This also explains why the CPU time required for the noncorrelated solution is larger than that required for the corresponding correlated solution.

Conclusions

The exact correlated and noncorrelated Monte Carlo formulations are very complicated for multidimensional systems. Solutions of these formulations are extremely difficult, if not impossible. However, by introducing the assumption of infinitesimal volume element, the approximate correlated and noncorrelated formulations are obtained, which are much simpler than the exact formulations. Consideration of different problems and comparison of different solutions reveals that the approximate and exact correlated solutions agree very well, and so do the approximate and exact noncorrelated solutions. But the two noncorrelated solutions have no physical meanings because they usually differ from the correlated solutions significantly. An accurate prediction of radiative heat transfer in any nongray and multidimensional system is possible by using the approximate correlated formulations developed in this study.

References

[1]Zhang, L., Soufiani, A., and Taine, J., "Spectral Correlated and Non-Correlated Radiative Transfer in a Finite Axisymmetric System Containing an Absorbing and Emitting Real Gas-Particle Mixture," *International Journal of Heat and Mass Transfer*, Vol. 31, No. 11, 1988, pp. 2261–2272.

[2]Menart, J. A., Lee, H. S., and Kim, T. K., "Discrete Ordinates Solutions of Nongray Radiative Transfer with Diffusely Reflecting Walls," *Journal of Heat Transfer*, Vol. 115, No. 1, 1993, pp. 184–193.

[3]Liu, J., and Tiwari, S. N., "Investigation of Radiative Transfer in Nongray Gases Using a Narrow Band Model and Monte Carlo Simulation," *Journal of Heat Transfer*, Vol. 116, No. 1, 1994, pp. 160–166.

[4]Siegel, R., and Howell, J. R., *Thermal Radiation Heat Transfer*, Hemisphere, New York, 3rd ed., 1992.

[5]Liu, J., "Radiative Interactions in Multi-Dimensional Chemically Reacting Compressible Flows," Ph.D. Dissertation, Old Dominion Univ., Norfolk, VA, 1994.

Spray Cooling Characteristics Under Reduced Gravity

Masaya Kato*
Keio University, Hiyoshi, Yokohama 223, Japan
Yoshiyuki Abe†
Electrotechnical Laboratory, Tsukuba, Ibaraki 305, Japan
and
Yasuhiko H. Mori‡ and Akira Nagashima‡
Keio University, Hiyoshi, Yokohama 223, Japan

Introduction

LIQUID spray cooling has been widely applied to many industrial processes requiring rapid and effective cooling. In space, spray cooling is expected to exhibit its outstanding potential in various thermal management systems[1] such as flash evaporators for use during re-entry, emergency cooling systems, quenching and cooling control systems for microgravity materials processing, etc. Spray cooling is, in general, thought to be rather insensitive to the variation in gravity. Nevertheless, there is experimental evidence that the heat transfer from a spray-cooled heater surface is dependent on its orientation, particularly in the transition region between the critical heat flux (CHF) point and the minimum heat flux (MHF) point, as well as in the higher surface-temperature region beyond the MHF point, and that the CHF is also under the influence of the surface orientation.[2] This fact suggests that gravity still plays some role in spray cooling.

The present study is the first attempt at evaluating the liquid spray cooling characteristics under reduced gravity conditions available in parabolic flights of an aircraft. The aircraft employed was an MU-300, a 15-m-long jet plane, which provided a reduced gravity condition of the order of 10^{-2} of the terrestrial gravity for approximately 20 s during each parabolic flight.

Experimental

The apparatus in the present experiments is schematically illustrated in Fig. 1. A liquid stored in a pressure vessel was displaced by pressurized dry nitrogen gas to generate liquid spray from the nozzle into the spray chamber, but no gas was introduced into the spray nozzle. The spray nozzle employed was a full-cone-type automobile fuel atomizer. The spray volume flux was adjusted by controlling the frequency of opening/shutting of the electromagnetic valve integrated into the nozzle, causing little change in droplet velocity. The droplet velocity was adjusted by controlling the liquid pressure in the pressure vessel. The liquid sprayed was either CFC-113 or water.

Figure 2 depicts the structure of the copper block used as the heated target to be spray-cooled. The copper block was heated up to a prescribed temperature (up to 320°C) by seven 750-W cartridge heaters embedded in the block, and then cooled down transiently by the liquid sprayed onto its nickel-plated surface, 19 mm in diameter, facing the nozzle. Ten parabolic flights were provided in a day, and the experiments started at the highest temperature and cooled down in the course of 10 parabolas. The total time for this operation was about 60 min.

Received June 24, 1994; revision received Aug. 25, 1994; accepted for publication Oct. 21, 1994.

*Graduate Student, Department of Mechanical Engineering.
†Senior Researcher, Energy Materials Section.
‡Professor, Department of Mechanical Engineering.

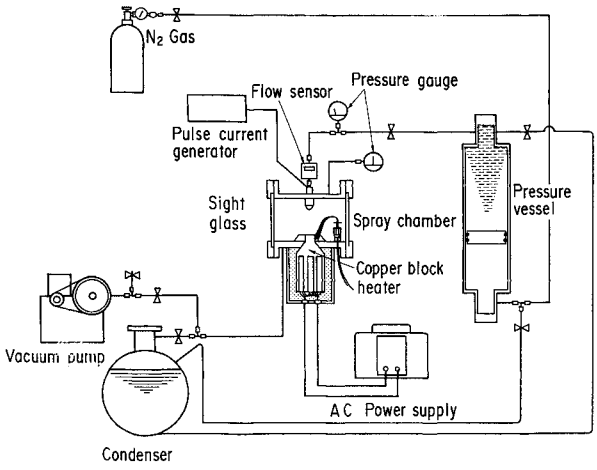

Fig. 1 Experimental apparatus for flight-experiment configuration.

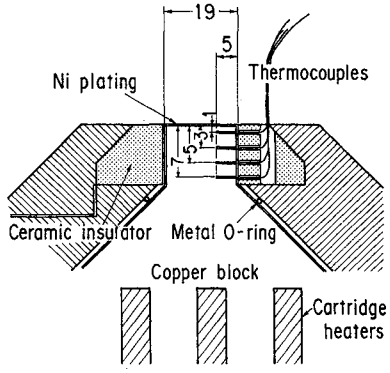

Fig. 2 Structure of copper block heater (scale in mm).

The instantaneous surface temperature and heat flux were evaluated from the temperature histories in the block detected by four 0.3-mm-diam chromel-alumel sheathed thermocouples that were soldered into 0.4-mm-diam holes, 5 mm in depth, drilled through the block parallel to the surface. The distance of each thermocouple from the surface was, 1, 3, 5, and 7 mm, respectively. The uncertainty in the surface temperature, defined as the deviation from the linear extrapolation of four thermocouples, was within ± 0.5 K for CFC-113 and within ± 1.1 K for water. The relative uncertainty in the determination of heat flux was less than $\pm 2\%$ in the vicinity of the CHF, but it increased up to $\pm 10\%$ in the low heat flux region and the transition region.

The distance between the nozzle and the heater surface was 100 mm. The distribution of spray volume flux over the surface was determined by using an array of droplets collecting pipes set in place of the copper block just 100 mm apart from the nozzle. It was found that water showed a rather uniform volume flux distribution, but CFC-113 gave a hollow-cone pattern.

The velocity distribution of spray droplets was measured with a laser Doppler velocimeter. For water the velocity distribution was found to be uniform within $\pm 10\%$. In contrast to this, CFC-113 showed a strong Gaussian distribution in which the maximum velocity along the axis of the spray was up to about 10 times the velocity of droplets falling on the periphery of the heated surface.

The size of water droplets was successfully determined by trapping them into a thin layer of silicone oil. For CFC-113 we tried to video-record the droplets sprayed through a fine slit under the nozzle, but this attempt was not successful in providing reliable data on the droplet size.

The temperature of the liquid to be sprayed was not particularly controlled except in a series of terrestrial experiments

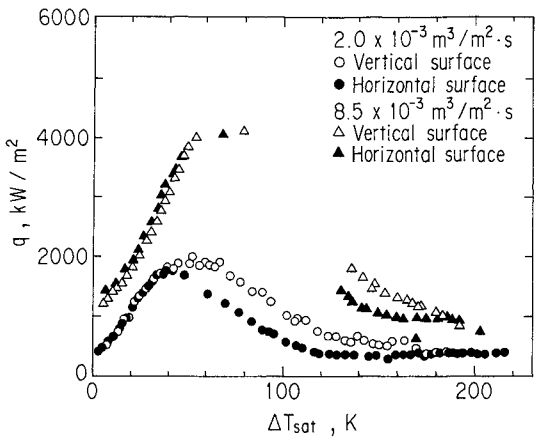

Fig. 3 Spray cooling characteristics of horizontal and vertical surface orientations for water (average droplet diameter 110 μm, liquid temperature 16.8–19.9°C, average droplet velocity 22.7 m/s).

in which the effect of liquid subcooling was studied. In the rest of the experiments, the liquid was sprayed nearly at the ambient temperature. The pressure in the spray chamber was always controlled at 0.101($\pm$0.002) MPa.

Results and Discussion

Effect of Surface Orientation

In advance of the parabolic flight experiments, we conducted some terrestrial experiments to investigate the dependency of the spray cooling characteristics on the orientation of the heated surface. The experiments were performed with the heated surface facing either horizontal upward direction or in a vertical direction.

Figure 3 compares the water-spray cooling characteristics for the two surface orientations in the form of the heat flux q, plotted against the surface superheat ΔT_{sat}. Irrespective of the spray volume flux, the CHF was slightly higher for the vertical surface than for the horizontal surface. The most significant difference in the q vs ΔT_{sat} relation depending on the orientation was noticed in the transition region, the transition region was displaced toward increasing ΔT_{sat}, typically by 20 K by the change from horizontal upward-facing to vertical of the orientation. The latter observation generally agrees with the results of Choi and Yao's experiments.[2]

Parabolic Flight Experiments

The present parabolic flight campaign continued for three days, and 10 parabolic flights were available in each day. The first day was devoted to the experiments with CFC-113. The experiments with water were conducted in the latter two days, changing the spray volume flux. To check the reproducibility of the experiments, the reference terrestrial data were taken in the aircraft before and just after the parabolic flights in the first and second days. All the reference experiments were performed while the heated surface was held parallel to the cabin floor so that it faced upward. For either fluid, a good reproducibility sufficient for the present purpose was confirmed.

Figure 4 compares the results for CFC-113 obtained in the reduced gravity and the terrestrial condition. Here we find that with the reduction in gravity the CHF decreased by about 10%, while the q vs ΔT_{sat} curve as a whole is shifted in the direction of lowering ΔT_{sat}. It should be particularly noted that the reduction in gravity affects the heat transfer more significantly in the transition region than in the low wall-superheat region below the CHF point.

The results for water at two different spray volume fluxes were presented in Figs. 5 and 6. These figures include the data obtained under the reduced and terrestrial gravities and also those obtained under elevated gravity conditions (1.5 and

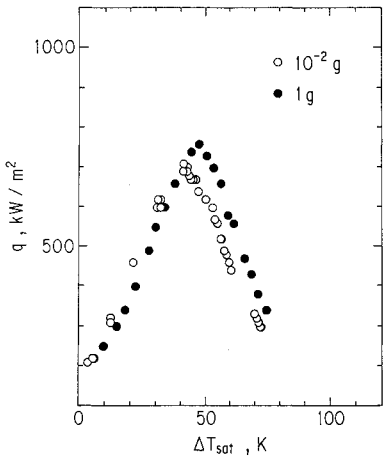

Fig. 4 Spray cooling characteristics for CFC-113 (spray volume flux 2.93 × 10^{-3} $m^3/m^2 \cdot s$, liquid temperature 11.4–13.0°C, droplet velocity 3.1–24.1 m/s).

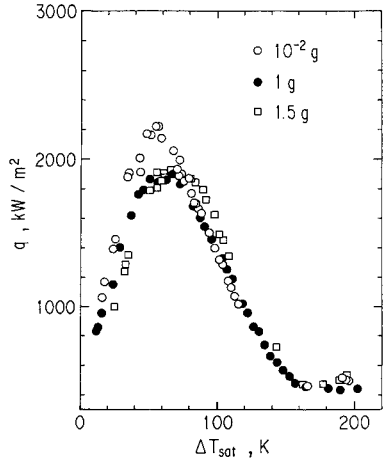

Fig. 5 Spray cooling characteristics for water at low spray volume flux (spray volume flux 2.51 × 10^{-3} $m^3/m^2 \cdot s$, liquid temperature 7.8–11.8°C, average droplet velocity 21.7 m/s, average droplet diameter 95 μm).

2 g) in the recovery and the entry periods of each parabolic trajectory of the aircraft. The results for the lower volume flux shown in Fig. 5 form a singular contrast to those for CFC-113 just shown. In Fig. 5 we notice an increase, instead of a decrease, in the CHF from the terrestrial level by about 15% with the reduction in gravity. The dependency of heat transfer on gravity appears to be more appreciable in the low wall-superheat region below the CHF point rather than in the region above the CHF point. Such difference in the gravity dependence of heat transfer between CFC-113 spray cooling and water spray cooling is possibly ascribed to the difference in physical properties between CFC-113 and water. However, it is also likely that the results shown in Figs. 4 and 5 reflect more or less the structural difference between the CFC-113 and water sprays as detected in the droplets velocities and the volume flux distributions. Thus, we cannot provide any definite interpretation of the apparent inconsistency between the results with CFC-113 and those with water.

At the higher spray volume flux the gravity dependency of heat transfer almost vanished (Fig. 6). This fact is easy to understand since the forced convective sensible heat transfer must become increasingly the dominant mechanism of heat removal from the heated surface with an increase in the spray volume flux.

In the low wall-superheat region below the CHF point, gravity is considered to affect the configuration of liquid pools,

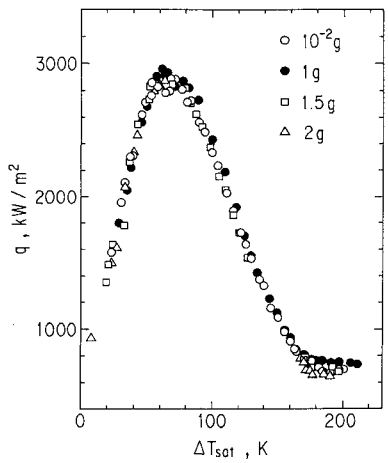

Fig. 6 Spray cooling characteristics for water at high spray volume flux (spray volume flux 5.35 × 10^{-3} $m^3/m^2 \cdot s$, liquid temperature 13.1–15.9°C, average droplet velocity 24.1 m/s, average droplet diameter 110 μm).

massive liquid drops, on the surface that is generated and developed by the coalescence of impinging droplets and unevaporated liquid films left on the heated surface, unless the spray volume flux is so high as to make the surface flooded by the liquid. A reduction in gravity presumably makes such liquid pools more globes, thereby increasing the dry surface area on which droplets can impinge directly. At present, this is no more than a hypothetical explanation of the enhancement of heat transfer in the low wall-superheat region recognized both in Figs. 4 and 5, but not in Fig. 6. Detailed observation of liquid/surface interactions through a transparent heating plate[3] are planned for the next parabolic flight experiments to clarify the point just discussed.

In the transition region, the reduction in gravity necessarily eliminates the chance of secondary impingement upon the surface of the droplets that have once rebounded from the heated surface. In addition, the vapor generated by the droplet evaporation does not remove from the heater surface in reduced gravity and possibly blankets the surface. These effects are presumably the cause of the lowering of q at each level of ΔT_{sat} with the reduction of gravity.

Concluding Remarks

First experiments on spray cooling under reduced gravity conditions have been conducted utilizing parabolic flights on an aircraft. The terrestrial reference experiments for horizontal upward and vertical heater orientations showed a noticeable effect of heater orientation, especially in the transition region. As far as the gravity effect is concerned, the present experiments brought the following new findings, some of which were unexpected:

1) A reduction in gravity yielded a reduction in the CHF for CFC-113, but an increase in the CHF for water.

2) Either fluid showed a heat transfer enhancement in the low heat flux region below the CHF by the reduction in gravity.

3) Heat transfer in the transition region of CFC-113 was significantly displaced toward decreasing ΔT_{sat} with a reduction of gravity.

4) The effect of gravity on the spray cooling characteristics was practically lost at high spray volume flux.

Since the spray pattern of CFC-113 and water was different from each other, however, it is not clear yet how to ascribe such different gravity effects observed for two fluids to either the physical properties of the fluids or the spray pattern. For reconfirming these results and clarifying the spray mechanism dominating or being explicit under reduced gravity condition, another series of parabolic flight experiments is schemed.

Acknowledgments

The authors appreciate the assistance of A. Kondo, a former undergraduate student of Keio University, in the present study. Thanks are also due to Diamond Air Service, Nagoya, Japan, for their faithful cooperation in the course of the parabolic flight experiments.

References

[1]Tilton, D. E., Ambrose, J. H., and Chow, L. C., "Closed-System, High-Flux Evaporative Spray Cooling," Society of Automotive Engineers, SAE-892316, Sept. 1989.

[2]Choi, K. J., and Yao, S. C., "Mechanism of Film Boiling Heat Transfer of Normally Impacting Spray," *International Journal of Heat and Mass Transfer*, Vol. 30, No. 2, 1987, pp. 311–318.

[3]Oka, T., Abe, Y., Mori, Y. H., and Nagashima, A., "Pool Boiling of *n*-Pentane, CFC-113 and Water Under Reduced Gravity," *Transactions of the American Society of Mechanical Engineers Journal of Heat Transfer* (to be published).

Simulation of Turbulent Heat Transfer in a Rotating Duct

Sandip Dutta,* Malcolm J. Andrews,† and Je-Chin Han‡
Texas A&M University, College Station, Texas 77843-3123

Introduction

We consider the turbulent heat transfer in a rotating duct, typical of cooling channels in a turbine blade. Figure 1 shows the geometry of the problem. Howard et al.[1] formulated a Coriolis turbulence production term for use in two-equation turbulence models without heat transfer. The predictions of Prakash and Zerkle[2] and Tekriwal[3] without a Coriolis turbulence production term in a k-ε turbulence model predict Nusselt numbers from trailing and leading surfaces that compare unevenly with experimental data. Dutta et al.[4] improved the predictions with the Coriolis modified turbulence term of Howard et al.[1] This Note presents further improvement of the work by Dutta et al.[4] and uses the published experimental heat transfer data of Wagner et al.[5] as a basis for comparison. Detailed consideration of the inlet effects, asymmetric distribution of turbulence due to rotation, and buoyancy effects are included.

Analysis

This work uses the high Reynolds number k-ε model of Launder and Spalding[6] incorporated into the PHOENICS computer code, and the nonequilibrium wall functions of Launder and Spalding[6] applied to near wall nodes. However, Coriolis and centrifugal buoyancy terms are added to the base model. Our modified model includes a Coriolis turbulence production, $P_C = 9\Omega\mu_t \cdot (\partial v_z/\partial x)$, and a buoyancy generated turbulence production, $P_b = \mu_t/Pr_t \cdot (\Omega^2 z)/T \cdot (\partial T/\partial z)$. Typical governing equations are given in Prakash and Zerkle,[2] while detailed equations are available in Dutta et al.[4]

Howard et al.[1] found that the Coriolis modified turbulence model increases the flow velocity and turbulence near the trailing side for radial outward flow in rotation, but reduces it near the leading side and stabilizes the flow. Their predictions were verified with experimental data in an unheated duct. We found that besides the Coriolis effect, in a heated duct rotational buoyancy due to temperature gradients accelerates the cooler fluid near the trailing edge and decelerates the warmer fluid near the leading surface. In the presence of a strong buoyancy force, the flow may separate near the leading side and the velocity and turbulence distribution may be entirely different from that in an unheated rotating duct.

The experimental setup of Wagner et al.[5] had a plenum chamber at the inlet of the test section. Their nonrotating flow measurements showed a fully developed turbulent flow at the inlet of the test section. However, no measurements with rotation were presented. The hydraulic diameter of the plenum chamber was larger than the hydraulic diameter of the actual test section. An increased hydraulic diameter means a larger cross-sectional flow area. Therefore, the axial flow velocity through the plenum chamber would be less than the axial flow velocity through the test section with an increase of the rotation number (Fig. 1) in the plenum chamber. Previous numerical predictions did not include the effect of the plenum chamber at the inlet. Prakash and Zerkle[2] and Tekriwal[3] started their computation domain from the start of heating and used fully developed turbulent profiles as the inlet condition. This approximation at the inlet condition resulted in a computation of a leading side Nusselt number that was higher than the trailing side, which is contrary to the experimental data. Rotating ducts are short in length and so inlet conditions need to be carefully prescribed. This work extended the computation domain upstream of the heated test section to allow flow development.

The cross-sectional area of the plenum chamber is 2.5 times that of the test section. To account for the area increase we have correspondingly increased the rotation speed by a factor of 4 along the unheated section of the duct ($z_0 < 0$ in Fig. 1) to maintain the same rotation number as in the plenum. Thus, we have a reasonable representation of the plenum chamber prior to the test section that better captures inlet profiles to the actual test section. This modification of the inlet condition

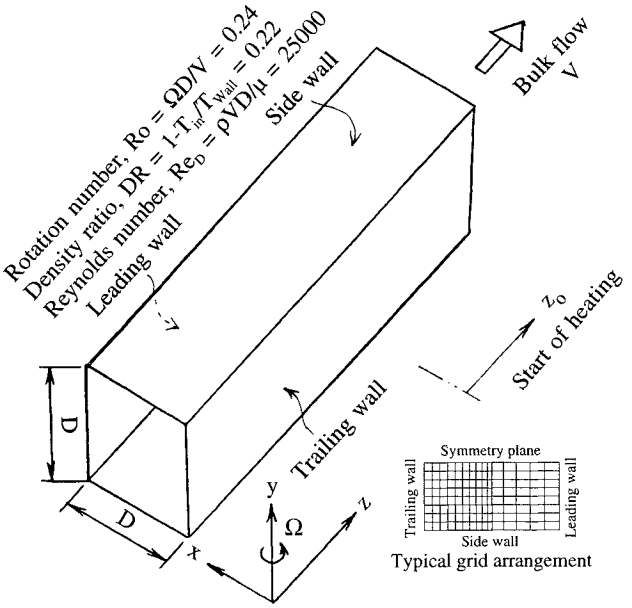

Fig. 1 Physical configuration and coordinate system.

Received Oct. 18, 1993; revision received July 5, 1994; accepted for publication Oct. 13, 1994.

*Graduate Student, Department of Mechanical Engineering. Student Member AIAA.

†Assistant Professor, Department of Mechanical Engineering. Member AIAA.

‡HTRI Professor, Department of Mechanical Engineering. Associate Fellow AIAA.